Supplementary material

Promoting effect of Cu on Pd applied to the hydrazine electro-oxidation and Direct Hydrazine Fuel Cells

Rudy Crisafully, Dryade Ferreira, Sabrina C. Zignani, Lorenzo Spadaro, Alessandra Palella, Simona Boninelli, José A. Dias [4] and José J. Linares

Figure S1 displays the XPS spectra of the different bimetallic materials. Signals corresponding to the Pd 3d and Cu 2p regions are presented, along with the deconvolution to estimate the outermost layer atomic composition, as well as the ratio of oxidation states. The estimation of the Cu oxidation state was according to the procedure described by Biesinger [1], without being able to separate the contribution for Cu(0) and Cu(I), given the very close binding energies.

PdC

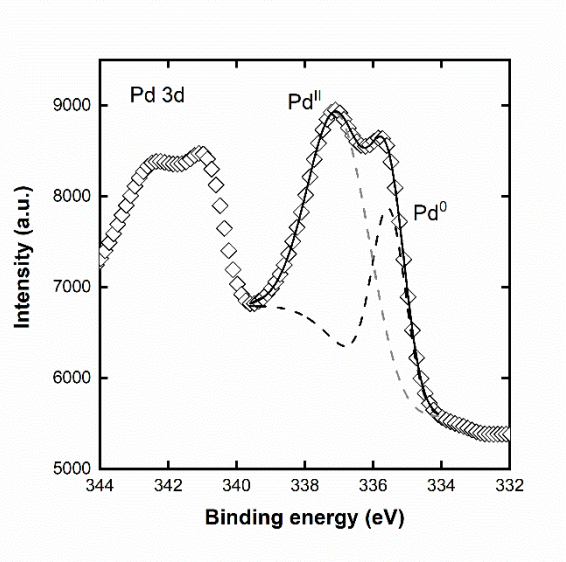

PdCu1C

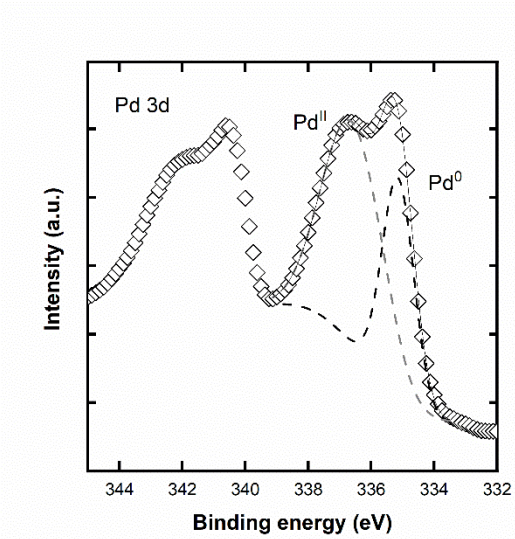
Pd 3d
Pd^{II}
Pd^{0}
Intensity (a.u.)
344
342
340
338
336
334
332
Binding energy (eV)

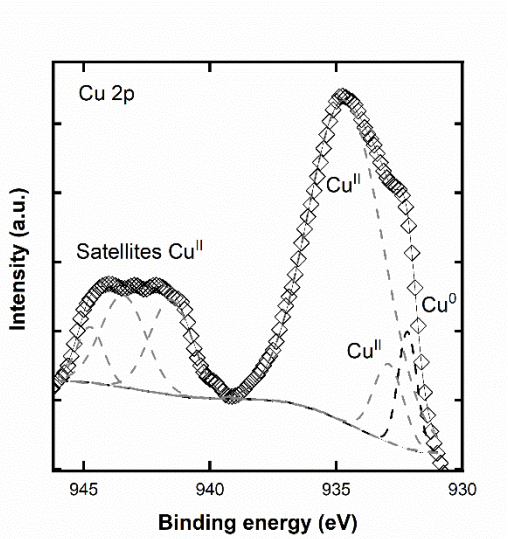
Cu 2p
Cu^{II}
Satellites Cu^{II}
Cu^{0}
Cu^{II}
Intensity (a.u.)
945
940
935
930
Binding energy (eV)

PdCu2C

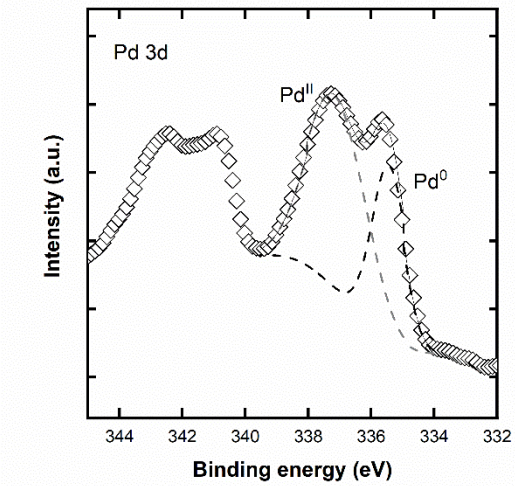
Pd 3d
Pd^{II}
Pd^{0}
Intensity (a.u.)
344
342
340
338
336
334
332
Binding energy (eV)

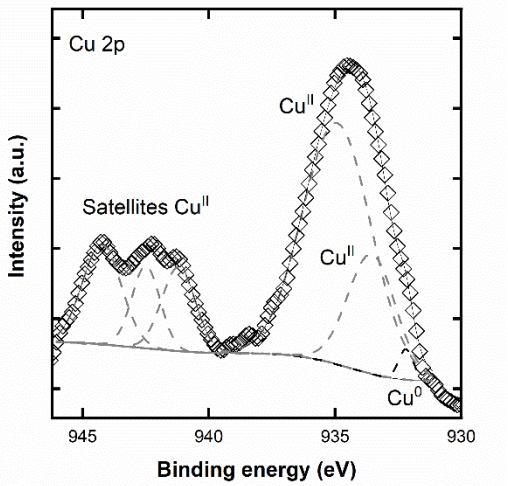
Cu 2p
Cu^{II}
Satellites Cu^{II}
Cu^{II}
Cu^{0}
Intensity (a.u.)
945
940
935
930
Binding energy (eV)

PdCu3C

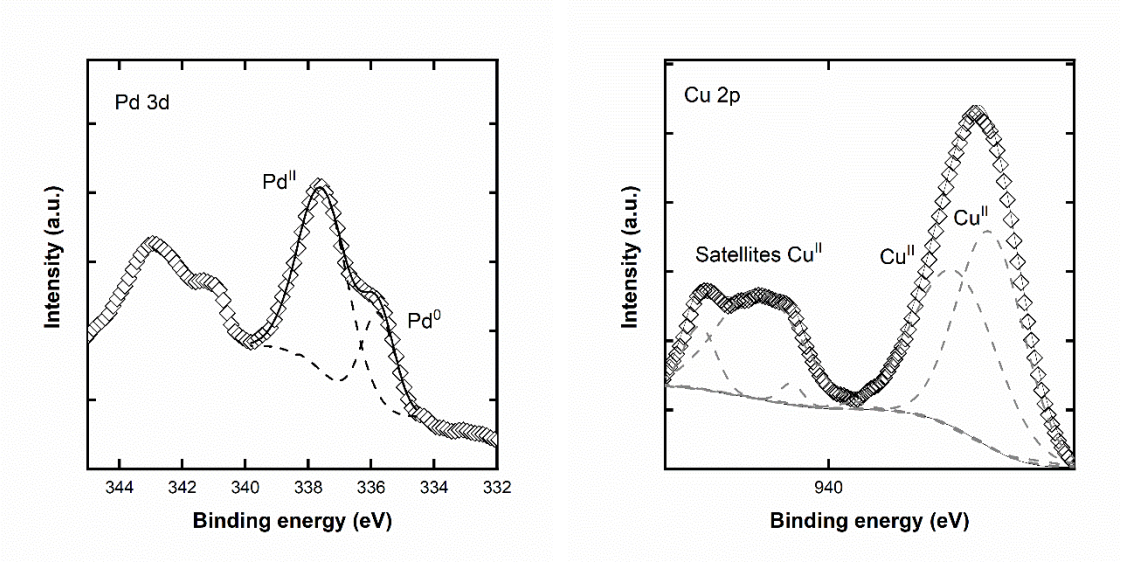

CuC

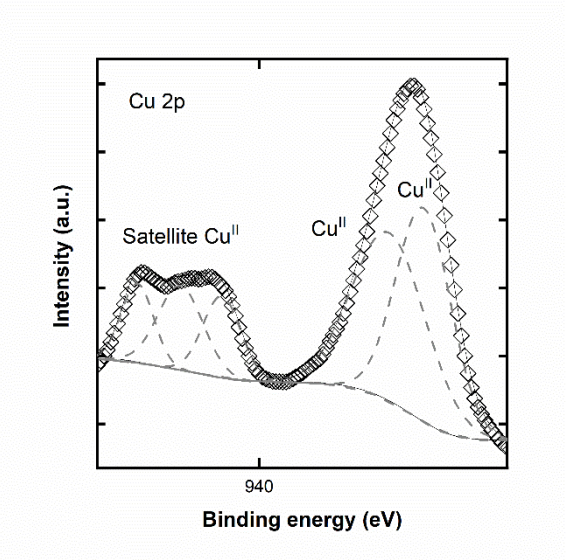

Figure S1. XPS spectra of the different electrocatalysts in the regions of Pd 3d and Cu2p.

Figure S2 presents the blank cyclic voltammograms (CV) of the electrocatalysts in KOH. The voltammograms of the PdCu1C and PdCu2C are, in overall terms, quite similar to PdC, as observed in the literature. They display the H adsorption/desorption region, along with the Pd oxide formation/reduction, with an increase in the signal of the region in which PdO is formed. Nevertheless, CuO can begin to interfere in this region in which Cu(II) (CuO and $Cu(OH)_2$ [2]) is formed. Indeed, The PdCu3C displays a combined profile between Pd and Cu, in which the larger fraction of Cu intensifies the signal in the "PdO formation region" (-0.2 to 0.0 V *vs*. mercury/mercury oxide, MMO) due to the oxidation of the superficial Cu. In the case of the CuC voltammogram, a first peak in the forward scan attributed to the Cu/Cu(I) (Cu_2O) (centered at ≈ -0.35 V *vs*. MMO) pair and a second larger peak attributed to the formation of Cu(II) species ($CuO/Cu(OH)_2$) [2] (centered at ≈ -0.1 V *vs*. MMO). The electrochemical active surface area (EASA)

can be estimated for Pd from the PdO reduction peak in the backward scan, around -0.2 V *vs.* MMO, according to Equation S1, where A_p is the corresponding area of the PdO reduction (see Figure S2), υ is the scan rate of the CV, Q_{PdO} is the integral Faraday charge for the PdO reduction (0.424 mC cm^{-2} of Pd) and m_{Pd} is the mass of Pd used [3]. Given that the CuC CV does not show a notorious signal in the PdO reduction region, we have tentatively estimated the EASA for all the materials. Table S1 collects the corresponding values. As can be seen, there is an increase in the EASA as the Cu content in the catalyst formulation increases. This can be associated with a decrease in particle size. These values will be used to normalize the hydrazine electrochemical oxidation reaction (HYEOR) voltamperometric curves.

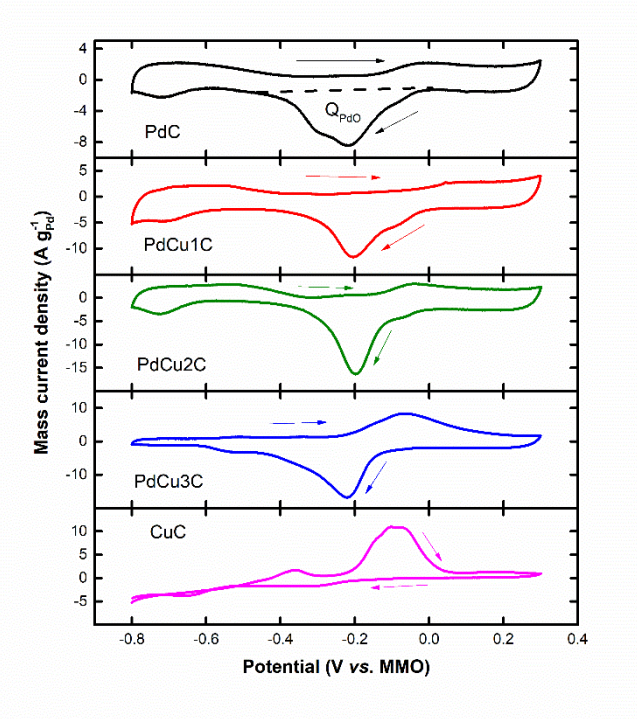

Figure S2. Blank cyclic voltammograms of the catalysts in 1 mol L^{-1} KOH.

Table S1. EASA of the different electrocatalysts.

Electrocatalyst	EASA (m^2 g^{-1} of Pd)
PdC	6.4
PdCu1C	7.2
PdCu2C	8.6
PdCu3C	9.6

Figure S3 shows the chronopotentiometric curves. The curves confirm the promotional effect that Cu exerts onto Pd for the HYEOR, especially for the PdCu2C, as widely discussed in the manuscript.

Finally, Figure S4 shows the scheme of the experimental setup used for the Direct Hydrazine Fuel Cells (DHFC) measurements. The DHFC operates in recirculation mode, returning the exhaust fuel to the hydrazine feed reservoir. Argon is used to purge the formed gases products, especially N_2 (m/z = 28), H_2 (m/z = 2), NH_3 (m/z = 17), and nitrogen oxides (N_2O, m/z = 44, NO, m/z = 30 and NO_2, m/z = 46). Only N_2 and H_2 are indeed detected, with no signals from ammonia and nitrogen oxides. Also, the m/z of argon (40) was monitored throughout the experiments.

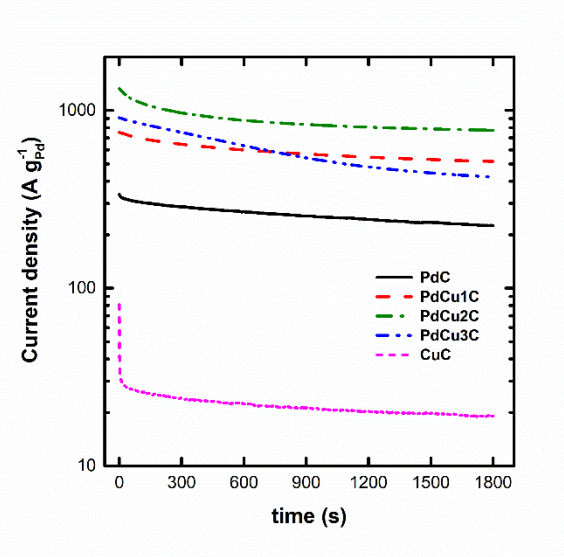

Figure S3. HYEOR chronoamperometric curves for the different electrocatalysts in 1 mol L^{-1} N_2H_4 and 1 mol L^{-1} KOH at 0.024 V *vs*. MMO.

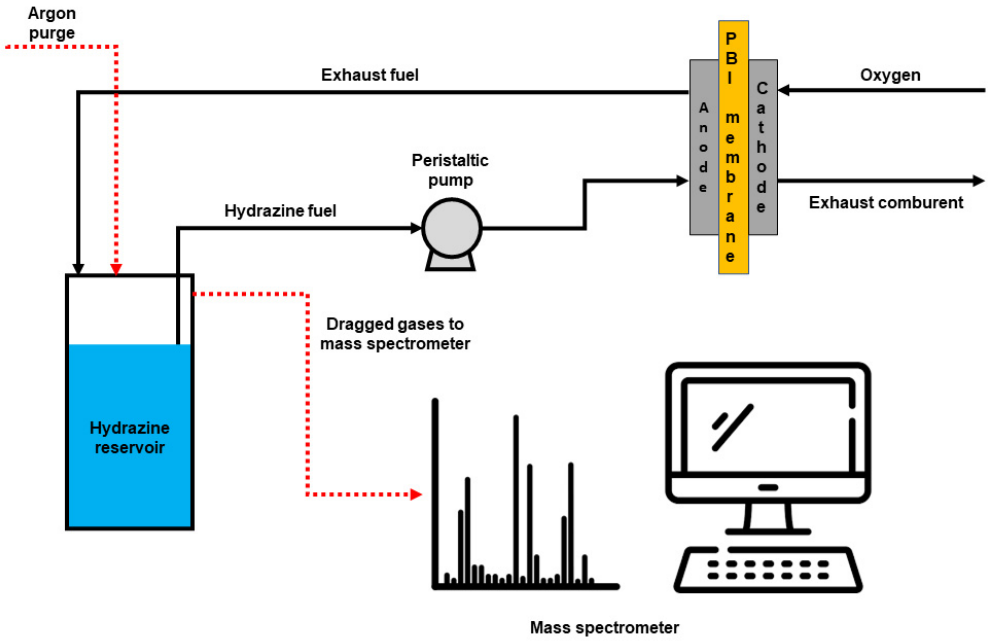

Figure S4. Experimental setup used to detect the HYEOR products.

References

1. Biesinger, M.C. Advanced Analysis of Copper X-Ray Photoelectron Spectra. *Surf. Interface Anal.* **2017**, *49*, 1325–1334, doi:10.1002/sia.6239.

2. Giri, S.D.; Sarkar, A. Electrochemical Study of Bulk and Monolayer Copper in Alkaline

Solution. *J. Electrochem. Soc.* **2016**, *163*, H252–H259, doi:10.1149/2.0071605jes.

3. Grdeń, M.; Łukaszewski, M.; Jerkiewicz, G.; Czerwiński, A. Electrochemical Behaviour of Palladium Electrode: Oxidation, Electrodissolution and Ionic Adsorption. *Electrochim. Acta* **2008**, *53*, 7583–7598, doi:10.1016/j.electacta.2008.05.046.